ESRF	**Experiment title: Macromolecular Crystallography at South-East Andalusia**	**Experiment number**: MX-2353
Beamline: ID30A-3	**Date of experiment**: From: 18 November 2021 / 19 November 2021	**Date of report**: 17/02/22
Shifts: 3	**Local contact(s)**: **Lindsay McGregor**	*Received at ESRF:*

Names and affiliations of applicants (* indicates experimentalists): Jose A. GAVIRA-GALLARDO*[1], Ana CAMARA-ARTIGAS[2], Sergio MARTINEZ-RODRIGUEZ*[3], Marina PLAZA-GARRIDO[2], Mari Carmen SALINAS-GARCIA[2], Carmen LOPEZ[1],

1. Laboratorio de Estudios Cristalográficos, IACT, CSIC-UGR, Spain.
2. Dpto. Química y Física, University of Almeria, Spain.
3. Dpto. de Bioquímica y Biología Molecular III e Inmunología, University of Granada, Spain.

Partial Report of MX2353 ID30B

This corresponds to the second report of our current proposal Mx2353 carried out remotely at ID30A-3. We send a Dewar wit 112 samples from the Granada (URG and CSIC) (Table 1) and some crystals in collaboration with the Almeria team.

Crystals from Granada CSIC & UGR (Table 1):

i) β-xylosidase from *Geobacillus stearothermophilus* (XynB2). Xylans are the most abundant polysaccharides forming the plant cell wall hemicelluloses, and they are degraded, among other proteins, by β-xylosidase enzymes. This enzyme has a clear biotechnogical application in the degradation of raw materials for the production of different monosaccharides, which are useful as fermentation sources or as alimentary supplements. New crystals (16) in different conditions to those obtained previously and soaked with different ligands have been measured. However, all diffracted poorly.

Future perspectives: New crystals have been produced, including a new mutant, to improve resolution and produced ligands complexess.

ii) Histidine ammonia-lyase from *Geobacillus kaustophilus* (HAL). This thermostable enzyme belongs to the superfamily of aromatic amino-acid ammonia lyases, with high applicability in the production of optically pure amino acids. We have embarked in the production of liganded-bound structures of this enzyme, for which no structural information is available at the PDB. We have also produced different active site-mutants (Y52F, R280K), in order to understand the molecular basis for the mechanism of this industrially relevant enzyme. We brought 37 crystals (ligand-free and soaked with different ligands), from which different datasets have been collected between 1.6-2.0 Å (e.g., SG I222, 1.7 Å, 105.5 108.4 112.2 90 90 90). Whereas clear densities have been ascertained in our different structures (see Figure 1), supporting a different mechanism to that proposed in the literature, further data is necessary to totally conclude our hypotheses.

Future perspectives: new crystals of HAL variants and new mutants have been produced, co-crystallized with different ligands, in order to improve our data.

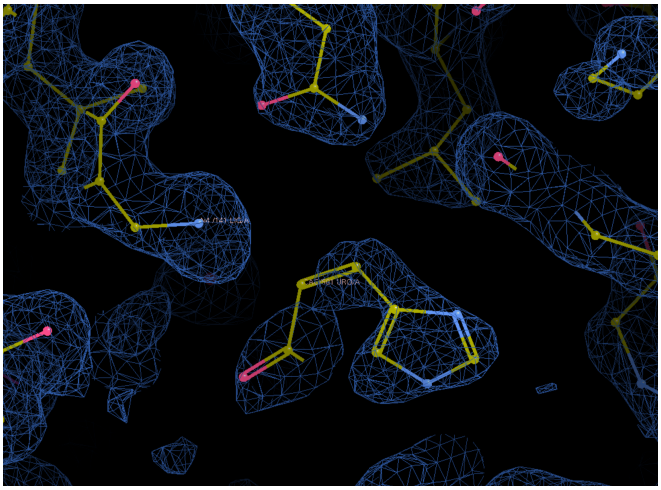

Figure 1. Structure of Y52F HAL mutant with bound uruconic acid in the catalytic centre

iii) Human bisphosphoglycerate mutase (BPGM). The level of 2,3-diphosphoglycerate (DPG), the allosteric ligand of hemoglobin, is controlled by BPGM. BPGM synthesizes DPG through its synthase activity and degrades it through its phosphatase activity. We have embarked in the structural characterization of BPGM and several of its mutants, in order to gain insights into erythrocytosis and hemolytic anemia. We measured the last 2 crystals obtained in different conditions, obtaining different datasets, the best at 1.84 Å (SG P21212, 98.8 130.6 38.6 90 90 90), including ligand-bound structures.

Future perspectives: Crystal improvement is ongoing together with the production of mutants associated to clinical variants have been produced.

iv) Acyl-phosphatase (AcP, QF3). AcP is one of the smallest enzymes known, catalyzing the hydrolysis of acylphosphates, both synthetic and of physiological relevance, such as benzoyl phosphate, aspartyl phosphate, and 1,3-bisphosphoglycerate. AcP family members have been proven to be very useful models for studies on protein folding and amyloid aggregation. We have brought 16 crystals of the AcP from *E. coli* (EcAcP), whose X-ray structure has not been determined previously. We have solved the structure of EcAcP from these datasets (2.84Å, SG C222, 40.4 81.8 63.6 90 90 90, actual R_{factor} and R_{free} of 28.8 and 36.4%, respectively)

Future perspectives: New crystallization experiments to improve the resolution are ongoing.

v) LysR-type transcriptional regulator (AdmX) from rizobacterium plymuthica. It has been shown that AdmX control the synthesis of the antibiotic andrimid in plants associated bacterium *Serratia plymuthica* A153. The environmental signals that bind to AdmX and modulate its action have been identified and can be classified a as agonists and antagonists. AdmX has been soaked with members of both classes and subject to crystallization. We test several crystals that did not diffract better than 3.0 A. Meanwhile we have used a modified poly-alanine model generated with AlfaFold2 to feed Arcimboldo-Borges and generate a solution further improved by manual reconstruction. The structure of the complex with IPA have been determined from data collected at ID23-1 and deposited at the PDB (ID. 7QEK) (Table 2). The manuscript, including the structure of AdmX bonded to IAA is in preparation.

Future perspectives: Complexes with some other ligands are being considered.

vi) PDZ3-PSD95. To study the polymorphism from this domain we have measured 25 crystals of PDZ3 domain. These crystals diffracted at high and medium resolution of ~1.5-2.0 Å belonging to one of the following SG: P3 (62 62 231 90 90 120) P222 (29 30 92 90 90 90), P1 (34 38 65 90 91 90), P1211 (29 87 32 90 93 90) P4 (30 30 92 90 90 90).

Table 1. Data collected by the CSIC-UGR-ALmeria.

Protein	Samples	Conditions	Cryo	Resolution
QF3	16	C31 Hampton I	15% GOL / No cryo	2.5-3.0
HAL and mutants	27	C3 HampII	15% GOL / No cryo	1.6-2.0
XynB2	16	C1	15% GOL / No cryo	---
BPGM	2	C9 HampI + agarose	15% GOL	2.0-3.0
PSD95	25	30% PEG 4000, 0.2 M AS, 0.1 M NaAc, pH 3.7-4.6	15% GOL	1.5-2.0
AdmX	16	C4	15% GOL	Poor diffraction.

Table 2. Data collection and refinement statistics. Statistics for the highest-resolution shell are shown in parentheses.

Ligand	**IAC**	**IPA**
PDB ID.	7QEJ	7QEK
Beam Line	XALOC (ALBA)	MASSIF-3 (ESRF)
Space group	P 21 21 2	P 21 21 21
Unit cell		
a, b, c (Å)	87.12 92.145 49.922	53.213 76.036 94.134
Resolution (Å)	63.31 - 1.81 (1.875 - 1.81)	35.26 - 2.25 (2.33 - 2.25)
Unique reflections	36996 (3667)	18464 (1838)
Multiplicity	4.2 (4.3)	4.5 (4.7)
Completeness (%)	98.85 (99.57)	98.43 (99.24)
I/σ_I	11.79 (1.43)	16.37 (1.54)
Wilson B-factor	30.58	49.44
R_{merge} (%)	6.44 (80.61)	5.50 (88.21)
CC(1/2)	0.998 (0.643)	0.999 (0.629)
Refinement		
R_{work}/R_{free} (%)	18.00 / 21.02	20.74 / 25.76
No. atoms	3587	3433
Protein	3417	3372
Ligands	44	31
Solvent	142	30
B-factor (Å^2)	41.55	60.91
R.m.s deviations		
Bond lengths (Å)	0.017	0.004
Bond angles (°)	1.36	0.79
Ramachandran (%)		
Favored (%)	98.26	96.52
Outliers (%)	0.00	0.00